Preparation of Azobenzene-Containing Amphiphilic Diblock Copolymers for Light-Responsive Micellar Aggregates

Guang Wang, Xia Tong, and Yue Zhao*

Département de chimie, Université de Sherbrooke, Sherbrooke, Québec, Canada J1K 2R1

Received July 30, 2004; Revised Manuscript Received September 15, 2004

ABSTRACT: Diblock copolymers composed of a side-chain liquid crystalline azobenzene-containing polymethacrylate and poly(*tert*-butyl acrylate) (PAzoMA-*b*-P*t*BA) were prepared using atom-transfer radical polymerization (ATRP). After subsequent selective hydrolysis of P*t*BA yielding poly(acrylic acid) (PAA), amphiphilic diblock copolymers of PAzoMA-*b*-PAA were obtained. Aggregation of either PAzoMA or PAA block occurs in solvents selective for one of the blocks. Adding water into dioxane solution of PAzoMA-*b*-PAA forms micellar aggregates due to the hydrophobic PAzoMA block. Under alternating UV and visible light illumination, reversible changes in micellar aggregates, for both core−shell micelles and vesicles, took place as a result of the reversible trans−cis photoisomerization of azobenzene mesogens in PAzoMA.

Introduction

In selective solvents, amphiphilic block copolymers can self-assemble to form micellar aggregates of various morphologies including star micelles, crew-cut micelles, rods, and vesicles.[1] A large number of works have been devoted to this topic in recent years and allowed the identification of many factors that contribute to determine the aggregate morphology.[1] These include the relative lengths of the hydrophobic and hydrophilic blocks and the nature of solvent to name only a few. Also, disruption of micellar aggregates, either permanently or reversibly, by means of external stimuli such as pH,[2] ionic strength,[3] and oxidation reaction[4] has been of much interest. This is explained by the potential to use polymer micellar aggregates for controlled release of substances such as drugs.[5] Although there are a few reports on the use of light as an external stimulus for small-molecule amphiphiles by incorporating the azobenzene chromophore into surfactant molecules,[6,7] we are not aware of reports on light-responsive micellar aggregates formed by amphiphilic block copolymers.

As part of our research on azobenzene-containing polymers and liquid crystals,[8−11] in this work we synthesized a series of azobenzene amphiphilic diblock copolymers that showed photoinduced reversible changes in morphology of micellar aggregates. The copolymer contains a hydrophobic side-chain liquid crystalline azobenzene polymethacrylate (PAzoMA) and the hydrophilic poly(acrylic acid) (PAA). As reported in the first part of the paper, it was prepared by synthesizing the diblock copolymer of PAzoMA-*b*-poly(*tert*-butyl acrylate) (P*t*BA) using atom-transfer radical polymerization (ATRP) and then selectively hydrolyzing P*t*BA to give PAzoMA-*b*-PAA. Although the hydrolysis degree of *t*BA groups was not 100%, the resulting PAA-*co*-P*t*BA random copolymer block became hydrophilic. For the sake of simplicity, the amphiphilic diblock copolymer is referred to as PAzoMA-*b*-PAA hereafter (see the chemical structure). The choice of a liquid crystalline (LC) polymethacrylate with mesogenic azobenzene moieties in the side group was based on the following consideration. Using the established method,[12] which consists of dissolving the polymer in a solvent common to both blocks and adding water to induce aggregation of the hydrophobic block, the insoluble PAzoMA would form the compact core of the micelle or the compact part in other micellar aggregates such as the bilayer membrane of vesicles. Since the LC order formed by azobenzene mesogens may persist inside the compact regions, on UV light irradiation, azobenzene in the elongated trans form is converted to the contracted cis form, which is known to destabilize the LC phase and induce a photochemical LC-to-isotropic phase transition.[13] If this happens, a strong disruption effect should be expected because it arises not only from the conformational change of azobenzene, but also from the phase transformation in the core or membrane regions. Since the azobenzene polymer in the isotropic state is more fluid than in the LC state,[14] such optically plasticized compact regions of PAzoMA by UV light may be deformed or broken up more easily due to, among others, a lower mechanical stability. As shown in the second part of the paper, experiments indeed found significant light-induced changes in the aggregate morphology of PAzoMA-*b*-PAA.

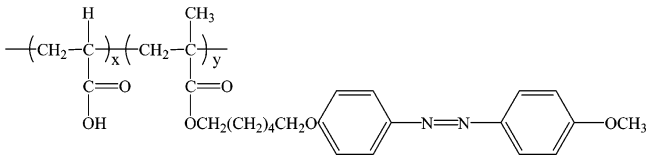

Experimental Section

Materials. *N*,*N*,*N*′,*N*′,*N*″-Pentamethyldiethylenetriamine (PMDETA), trimethylsilyl iodide (TMSI), copper bromide, ethyl 2-bromoisobutyrate, and 2,6-di(*tert*-butyl-4-methyl)phenol were purchased from Aldrich and used without further purification. THF was refluxed with sodium and distilled. *tert*-Butyl acrylate (Aldrich) was distilled with 2,6-di(*tert*-butyl-4-methyl)-phenol as inhibitor before use.

Synthesis of PAzoMA-*b*-P*t*BA. The macroinitiator of poly(*tert*-butyl acrylate) (P*t*BA-Br) was prepared following the literature method using CuBr complexed with PMDETA as catalyst and ethyl bromoisobutylate as initiator.[15] The two

* To whom correspondence should be addressed. E-mail: yue.zhao@usherbrooke.ca.

10.1021/ma048416a CCC: $27.50
Published on Web 10/28/2004

Table 1. Characteristics of Diblock Copolymers before and after Hydrolysis

	PAzoMA-*b*-P*t*BA[a]			PAzoMA-*b*-PAA[b]			
sample no.	M_n (GPC)	M_w/M_n (GPC)	M_n (NMR)	M_n (GPC)	M_w/M_n (GPC)	M_n (NMR)	hydrolysis degree (%)
1	22 100	1.28	16 400	20 100	1.58	14 500	72
2	23 000	1.28	23 500	19 600	1.39	21 000	90
3	23 100	1.31	19 100	21 100	1.74	17 100	63 (60)[e]
4	27 500	1.30	25 700	25 900	1.92	23 000	54
5	35 900	1.29	28 100	27 200	1.69	26 300	57
6	45 000	1.38	38 000	32 500	1.51	34 200	32 (34)
P*t*BA-Br (1)[c]	6 700	1.10					
P*t*BA-Br (2)[d]	8 700	1.19					

[a] Diblock copolymers before hydrolysis. [b] Diblock copolymers after hydrolysis. [c] Used for samples 1−5. [d] Used for sample 6. [e] Values in parentheses were estimated from ^{13}C NMR.

P*t*BA-Br macroinitiators obtained have $M_n = 6700$ with $M_w/M_n = 1.10$ and $M_n = 8700$ with $M_w/M_n = 1.19$, respectively (GPC with polystyrene standards). The monomer AzoMA, namely, 6-[4-(4-methoxyphenylazo)phenoxy]hexyl methacroylate, was also synthesized using the documented procedure.[16] Diblock copolymers of PAzoMA-*b*-P*t*BA were then obtained through P*t*BA-Br-initiated polymerization of AzoMA. Details on the synthesis of one sample, PAzoMA-*b*-P*t*BA (3) (Table 1) are given below as an example. P*t*BA-Br (0.2 g), AzoMA (0.5 g), and CuBr (5 mg) were charged to a round-bottom flask with a stir bar. After the flask was degassed and backfilled with nitrogen three times, THF (1.2 mL) was added to dissolve the compounds. The mixture was stirred until a homogeneous solution was formed. Then PMDETA (20 mg) was added, and the solution was stirred until the Cu complex had formed, which could be noticed as the color of the solution turned light green. The flask was frozen in liquid nitrogen, and a vacuum was applied. After three freeze−pump−thaw cycles, the flask was sealed and placed in an oil bath at 60 °C for 14 h. The reaction mixture was diluted with THF and passed through an alumina column. The polymer was purified by precipitation in methanol three times and then collected and dried in a vacuum oven. $M_n = 23\,100$ and $M_w/M_n = 1.31$. Other diblock copolymers in the series (Table 1) were prepared under the same conditions, while the feed ratio of AzoMA to P*t*BA-Br was varied to give rise to different compositions.

Preparation of PAzoMA-*b*-PAA through Selective Hydrolysis. With PAzoMA-*b*-P*t*BA undergoing the hydrolysis reaction, a selective cleavage of *tert*-butyl groups is expected because the hydrolysis of *tert*-butyl ester should be much easier than the hydrolysis of the ester group with azobenzene mesogen. The reaction was carried out using the literature method.[17] As an example, PAzoMA-*b*-P*t*BA (3) (0.2 g) was dissolved in dichloromethane (10 mL) in a flame-dried round-bottom flask connected to the N_2 line. To the solution was then added TMSI (1.2 mol equiv to *tert*-butyl ester groups). The mixture was stirred under nitrogen for 40 min. After the reaction, the solvent and excess TMSI were removed under reduced pressure. The solid remaining was dissolved in THF, and the solution was added dropwise into HCl solution (0.1 M, 100 mL) containing 1 wt % $Na_2S_2O_5$ under stirring. The mixture was stirred for 1.5 h, and the solid was collected by filtration and washed with water three times. Afterward, the solid was dissolved in THF, and the hydrolyzed polymer was precipitated in cold ethyl ether three times. $M_n = 21\,100$ and $M_w/M_n = 1.74$.

Preparation of Micellar Aggregates. Micellar aggregates of PAzoMA-*b*-PAA were prepared by adding water in dioxane solution of the polymer. Two initial polymer concentrations of 1.0 and 5.0 mg/mL were used for two different diblock copolymers, respectively. In the case of 1.0 mg/mL, water was added slowly with stirring. To investigate the effects of irradiation, the micellar solution, placed in a small vial, was exposed to either UV light for 10 min or visible light for 3 min; then 10-fold water was added to quench the aggregates. To prepare samples for scanning (SEM) and transmission electron microscope (TEM) observations, one drop of the diluted solution was cast on a silicon wafer (for SEM) or carbon-coated copper grid (for TEM) and dried at room temperature. In the case of 5.0 mg/mL, after slowly adding 26 wt % of water into the dioxane solution, more water was added quickly to dilute the solution, reaching a turbidity of about 1.3 measured at 700 nm. UV and visible light irradiation of the solution lasted 10 min. The samples cast for SEM or TEM observations, before and after light illumination, were quenched immediately after casting with liquid nitrogen and then freeze-dried (−50 °C).[18]

Characterizations. Diblock copolymers before and after hydrolysis were characterized using a number of techniques. ^1H NMR spectra were recorded on a Bruker Spectrometer (300 MHz, AC 300). Molecular weights and polydispersities were measured by gel permeation chromatography (GPC) using a Waters system equipped with a refractive index and a photodiode array detector. For GPC measurements, THF was used as the eluent (elution rate, 0.5 mL/min) and polystyrene standards used for calibration. Thermal phase transitions were examined using a Perkin-Elmer DSC-7 differential scanning calorimeter with a heating or cooling rate of 10 °C/min. Infrared and UV−vis spectra were recorded on a Bomem-MB200 FTIR and a Hewlett-Packard 8452A diode array spectrophotometer, respectively. To investigate the effects of UV and visible light irradiation on micellar aggregates, a UV−vis curing system (Novacure) combined with UV and visible filters was utilized to generate UV (∼360 nm, 35 mW/cm^2) and visible light (∼440 nm, 39 mW/cm^2). The turbidity of micellar solutions was measured at 700 nm, which was far from absorption of the azobenzene chromophore, using the same UV−vis spectrophotometer.[12] Micellar aggregates were examined using a Hitachi H-7500 transmission electron microscope (TEM) operating at 80 KV and a Hitachi S-4700 Field-Emission-Gun scanning electron microscope (SEM) operating at 3 KV.

Results and Discussion

Synthesis and Characterization of Block Copolymers. Using ATRP, the P*t*BA-Br macroinitiators of narrow polydispersity were used to grow the second block of PAzoMA of different lengths. The polydispersity of the resulting diblock copolymer of PAzoMA-*b*-P*t*BA increased slightly with respect to the macroinitiator. It further increased after the selective hydrolysis reaction, yielding the amphiphilic diblock copolymer of PAzoMA-*b*-PAA. ^1H NMR spectroscopy was the main tool used to analyze the block copolymers both before and after the hydrolysis reaction. First, it was used to estimate the composition of each block copolymer, from which a NMR-based number-average molecular weight of the polymer was determined (using the GPC value of P*t*BA-Br). Second, ^1H NMR was used to monitor the hydrolysis reaction that should selectively remove *tert*-butyl groups from the P*t*BA block. Third, the amphiphilic behavior of PAzoMA-*b*-PAA in different solvents was examined by means of ^1H NMR. Before discussing specific examples, Table 1 summarizes the main characteristics of a series of PAzoMA-*b*-P*t*BA and the resulting PAzoMA-*b*-PAA diblock copolymers. In the text, the samples

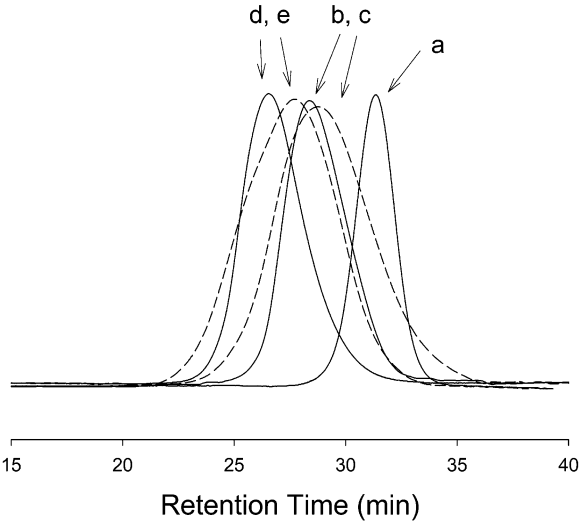

Figure 1. GPC curves of the macroinitiator and two diblock copolymers before and after hydrolysis: (a) P*t*BA-Br, (b) PAzoMA-*b*-P*t*BA (2), (c) PAzoMA-*b*-PAA (2), (d) PAzoMA-*b*-P*t*BA (5), and (e) PAzoMA-*b*-PAA (5).

are differentiated from each other by a number in parentheses in their acronyms. For example, for sample 2 in Table 1, the diblock copolymer before and after hydrolysis is denoted as PAzoMA-*b*-P*t*BA (2) and PAzoMA-*b*-PAA (2), respectively.

Figure 1 shows the GPC curves of the macroinitiator P*t*BA-Br (1), two PAzoMA-*b*-P*t*BA samples, and their corresponding PAzoMA-*b*-PAA amphiphilic block copolymers after hydrolysis. It is clear that growth of the PAzoMA block from the macroinitiator proceeded in a controlled way. After the hydrolysis reaction, the average molecular weights of the copolymers are decreased slightly and their polydispersity increased. This was found for all samples listed in Table 1. Even though it is difficult to establish any quantitative correlation between the decrease in molecular weight and the degree of hydrolysis, the results are consistent with removal of bulky *tert*-butyl groups from the polymer. Despite the larger polydispersity resulting from the hydrolysis reaction, the results clearly indicate the absence of any severe side reactions such as cross-linking and chain scission under the conditions used.

To demonstrate the selective hydrolysis of PAzoMA-*b*-P*t*BA and the amphiphilic nature of the resulting diblock copolymer, Figure 2 compares the ^{1}H NMR spectrum of PAzoMA-*b*-P*t*BA (3) in deuterated chloroform (spectrum 1), which is a good solvent for the two blocks before hydrolysis, with that of PAzoMA-*b*-PAA (3) in deuterated THF (spectrum 2), which is a good solvent for both blocks after hydrolysis. The NMR spectra of PAzoMA-*b*-PAA (3) in chloroform and DMSO are also given (spectra 3 and 4, respectively) to show the aggregation of either block depending on the solvent. Two observations can be made. First, before hydrolysis of sample 3 in Table 1, based on M_n (NMR), the mass ratio of PAzoMA to P*t*BA is about 1.9 corresponding to a ratio of about 0.6 for the number of AzoMA units over that of *t*BA units (the ratio of *y*/*x* in the chemical structure shown in Figure 2). Although an accurate analysis is difficult because of the overlap of peaks in the 1−2 ppm region, the most prominent peak near 1.4 ppm is mainly assigned to the 9 H of the *tert*-butyl group in *t*BA and 8 of the 12 H in the alkyl chain spacer in AzoMA. If the selective hydrolysis of P*t*BA was 100%

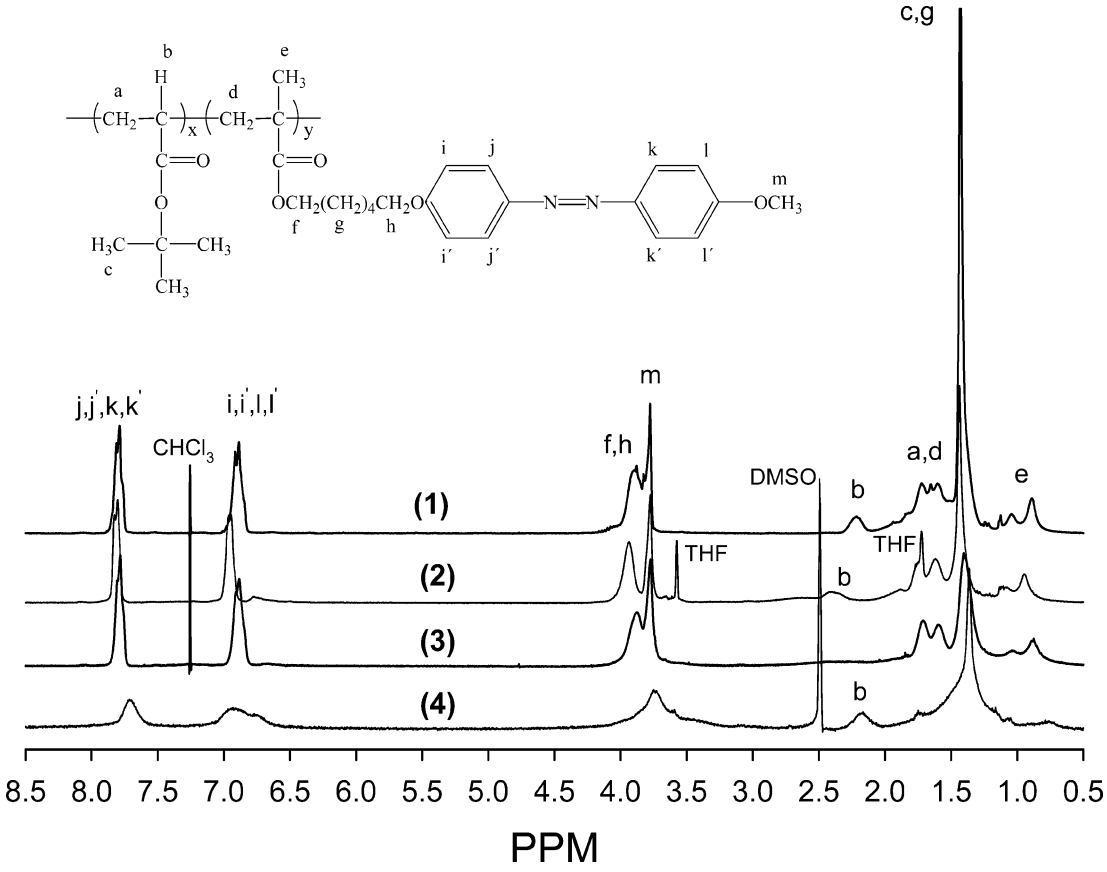

Figure 2. ^{1}H NMR spectra of PAzoMA-*b*-P*t*BA (3) in chloroform (spectrum 1), PAzoMA-*b*-PAA (3) in THF (spectrum 2), PAzoMA-*b*-PAA (3) in chloroform (spectrum 3), and PAzoMA-*b*-PAA (3) in DMSO (spectrum 4).

efficient, the area of this peak should drop by about 65% with respect to the peaks of phenyl protons of azobenzene of the PAzoMA block. From the spectrum of PAzoMA-*b*-PAA in THF-d_8 (spectrum 2), it is seen that hydrolysis was substantial though not 100%. This analysis is, of course, based on the assumption that the hydrolysis reaction did not affect the PAzoMA block, which is reasonable judging from spectra 1 and 2. Indeed, the peak at about 2.2 ppm in $CDCl_3$ and 2.4 ppm in THF-d_8, which comes only from the P*t*BA block, is particularly useful for the analysis since it should not be affected by the degree of cleavage of *tert*-butyl groups. The area of this peak is essentially unchanged with respect to the phenyl peaks in the 6.5−8 ppm region, before and after hydrolysis, indicating that the hydrolysis reaction did not remove azobenzene mesogenic groups. The hydrolysis degree of *tert*-butyl ester groups as estimated from ^{1}H NMR was given in Table 1 for all samples. For the two samples used to investigate light-responsive micellar aggregates, the hydrolysis degree was also estimated from ^{13}C NMR, yielding very similar results (Table 1).

Second, the amphiphilic behavior of PAzoMA-*b*-PAA (3) is also reflected by the ^{1}H NMR spectra in different solvents. In $CDCl_3$ (spectrum 3), the signature peak of PAA near 2.2 ppm is absent while the peaks of PAzoMA are visible and comparable to those in THF-d_8 (spectrum 2). This indicates the selective solvation of the PAzoMA block and aggregation of the PAA block in chloroform. The opposite occurs in DMSO-d_6 (spectrum 4); while the peak of PAA near 2.2 ppm reappears, those of PAzoMA are broadened with diminished intensity. In this more polar solvent, the PAA block is preferentially dissolved and the PAzoMA block aggregates.

Regarding hydrolysis of P*t*BA in the diblock copolymers, having performed a number of experiments varying different parameters such as reaction time, solvent, and polymer concentration, the results in Table 1 are the best we have achieved, which was obtained using the conditions described in the Experimental Section. It was observed that when the amount of trimethylsilyl iodide (TMSI) was higher than about 1.4 mol equiv of *t*BA, the molecular weight of the copolymer after hydrolysis rose drastically, suggesting the occurrence of cross-linking or coupling side reactions. Whereas when the amount of TMSI was reduced to lower than 1.2 mol equiv, no effective hydrolysis took place. These observations suggest that the PAzoMA block rendered clean hydrolysis of the P*t*BA block difficult to achieve. However, it should be emphasized that despite partial hydrolysis, selective cleavage of *tert*-butyl groups is evidenced by ^{1}H NMR spectroscopy as discussed above, which transforms all PAzoMA-*b*-P*t*BA diblock copolymers in Table 1 to amphiphilic diblock copolymers, including PAzoMA-*b*-PAA (6), which has the lowest hydrolysis degree of about 30%. Another piece of information that shows the conversion of P*t*BA to PAA came from infrared spectroscopy. Figure 3 compares the spectra of PAzoMA-*b*-P*t*BA (2) and PAzoMA-*b*-PAA (2). The block copolymer after hydrolysis displays the characteristic absorption bands of intermolecular carboxylic acid dimer, which are absent before hydrolysis. These are the broad band around 3000 cm^{-1} (O−H) and the band appearing at 1700 cm^{-1} (C=O) for PAzoMA-*b*-PAA.[19] Before hydrolysis, the band at 1727 cm^{-1} is the sum of the carbonyl bands from both PAzoMA and P*t*BA. After hydrolysis, this band splits into two components, the new one at 1700 cm^{-1} arising from hydrogen-bonded carboxylic acid dimer, indicated by an arrow in Figure 3, and the one remaining at about 1725 cm^{-1} contributed by the PAzoMA block as well as free acid and residual *tert*-butyl ester groups in the microphase-separated PAA. This also explains why the band at 1700 cm^{-1} is not as dominant as in pure PAA.

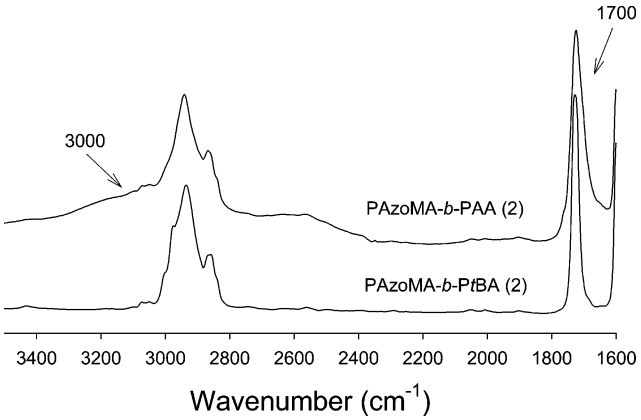

Figure 3. Infrared spectra of PAzoMA-*b*-P*t*BA (2) and PAzoMA-*b*-PAA (2).

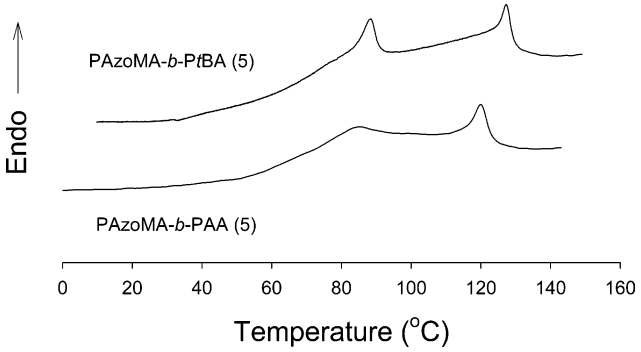

Figure 4. DSC heating curves (second scan) for PAzoMA-*b*-P*t*BA (5) and PAzoMA-*b*-PAA (5).

The liquid crystallinity of the PAzoMA block is preserved after the hydrolysis reaction, as can be seen from the DSC heating curves in Figure 4. PAzoMA is known to have a smectic (S) and nematic (N) phase.[20,21] On heating PAzoMA-*b*-P*t*BA (5) and PAzoMA-*b*-PAA (5), the two mesophase transition endothermic peaks, S-to-N and N-to-isotropic (I), are visible after a T_g of the PAzoMA block near 65 °C. However, the mesophase transition temperatures T_{SN} and T_{NI} are decreased from 88 and 127 °C before hydrolysis to 83 and 119 °C after hydrolysis with the associated enthalpies, ΔH_{SN} and ΔH_{NI}, also reduced from about 1.1 and 1.2 J/g to 0.5 and 1.1 J/g. This is likely to be caused by the widened distribution of molecular weights for PAzoMA-*b*-PAA and probably an increased interfacial interaction between PAzoMA and PAA microdomains as compared with PAzoMA-*b*-P*t*BA. Similar mesophase transition temperatures were observed for the other amphiphilic PAzoMA-*b*-PAA diblock copolymers in Table 1. Note also that the P*t*BA-Br macroinitiator has a low T_g at about 31 °C, while the T_g of the P*t*BA block in PAzoMA-*b*-P*t*BA (5) is not clearly discernible because of its low weight fraction. In PAzoMA-*b*-PAA (5), T_g of the PAA block should increase to around 90 °C, likely overlapped by the S-to-N phase transition peak.

Light-Responsive Micellar Aggregates. As mentioned in the Introduction, if micelles are formed with

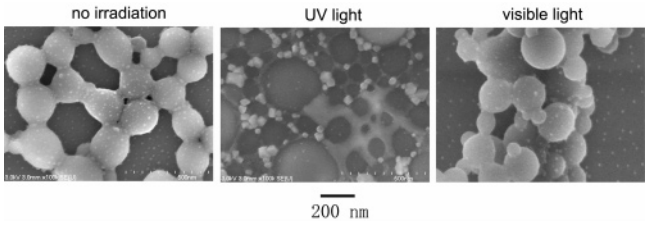

Figure 5. SEM images of coexisted core−shell micelles and large micelle-like aggregates of PAzoMA-*b*-PAA (3) formed by adding water in dioxane solution: before irradiation and after UV and visible light irradiation. The initial polymer concentration was 5.0 mg/mL.

the PAzoMA block forming the compact core, the LC order between azobenzene mesogens may remain in the aggregation. These micelles should respond to UV light by undergoing the trans−cis isomerization-induced photochemical phase transition,[13] which turns the LC state inside the micelle core into the isotropic state. If this happens, the polymeric micelle may not necessarily fall apart but the mechanical stability of the optically plasticized micelle should be weakened. To investigate possible light-induced changes, we first prepared micellar solutions of PAzoMA-*b*-PAA (3) whose hydrophobic block contains about 31 units of AzoMA and whose hydrophilic block is composed of 33 units of AA and 19 units of *t*BA. The polymer was dissolved in dioxane with an initial concentration of 5 mg/mL. After addition of water, the micellar solution was first exposed to UV light for 10 min under stirring for the trans−cis photoisomerization of azobenzene mesogens. Once the UV light was turned off, the solution was cast on either silicon wafer or copper grid and the aggregates quenched and freeze-dried. To examine the reversibility of light-induced changes in the aggregate morphology, the UV-irradiated solution was subsequently exposed to visible light for 10 min under stirring for the cis−trans backisomerization. After visible light was turned off, samples were prepared under the same conditions for SEM and TEM observations.

Figure 5 shows representative SEM images of the micellar aggregates prepared by slow addition of 26 wt % water in dioxane solution followed by dilution as described in the Experimental Section. In the initial solution, polymeric core−shell micelles (∼15 nm) were found to coexist with large micelle-like aggregates (most in the 200 nm range). After UV light irradiation, the change in morphology is significant. While polymeric micelles could still be observed, the number was diminished. The larger aggregates were severely disrupted, and the number reduced too. After subsequent visible light irradiation, the morphology essentially returned back to that of the initial solution with polymeric micelles coexisting with large spherical aggregates. Similar morphological changes were observed on TEM. The large spherical aggregates may simply be the phase-separated polymer under the used conditions. This photoinduced reversible change in morphology of the aggregates is also reflected by a reversible change in turbidity of the micellar solution upon alternating UV and visible light irradiations, as shown in Figure 6 for a number of irradiation cycles. For this experiment the turbidity was measured after 10 min irradiation of the solution under mild stirring outside the sample compartment of the spectrophotometer. The decrease in turbidity under UV light is in agreement with the observed decrease in the number of aggregates. On

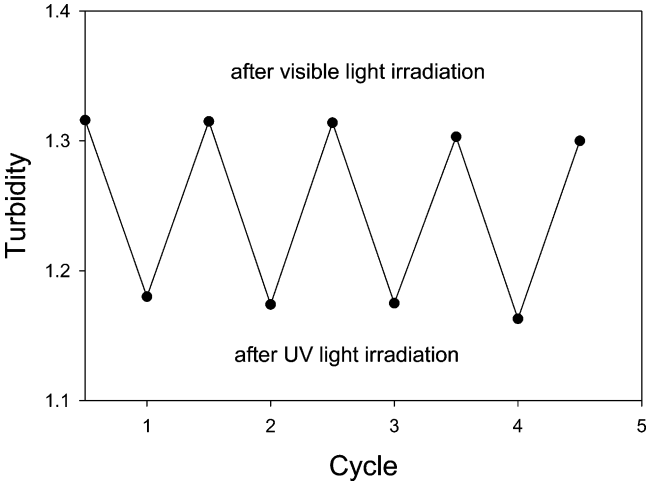

Figure 6. UV and visible light-induced reversible change in turbidity of the micellar solution containing the micellar aggregates shown in Figure 5. The turbidity was measured at 700 nm.

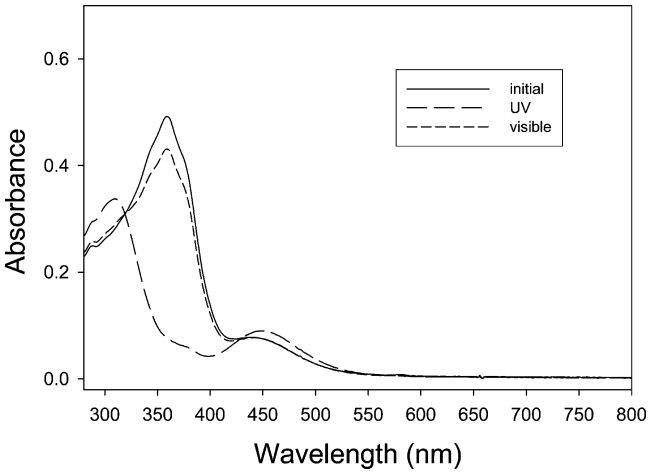

Figure 7. UV−vis spectra of PAzoMA-*b*-PAA (3) in dioxane: (∼4.3 × 10^{-3} mg/mL) before irradiation and after UV and visible light.

visible light irradiation, the turbidity increased to the initial level, implying reformation of micellar aggregate as before the UV light exposure.

The reversible trans−cis photoisomerization of azobenzene mesogens in PAzoMA is responsible for the observed reversible change in morphology of the micellar aggregates. Although the optical density of the micellar solution in the 300−500 nm region was too high to assess the photoisomerization due to the high content of azobenzene mesogens, the efficiency of the process can be seen from the UV−vis spectra of PAzoMA-*b*-PAA (3) in dilute dioxane solution (∼4.3 × 10^{-3} mg/mL) as shown in Figure 7. The occurrence of the trans−cis isomerization on UV light exposure is noted from the drop of the absorption maximum of *trans*-azobenzene mesogens at about 360 nm ($\pi-\pi^*$ transition), which is accompanied by the absorption band of *cis*-azobenzene near 450 nm ($n-\pi^*$). The concentration of *cis*-azobenzene at the photostationary state is almost 100%. On visible light irradiation, *cis*-azobenzene returns to *trans*-azobenzene. It is seen that the recovered absorbance of *trans*-azobenzene is slightly lower than that before irradiation. However, the change in absorbance became completely reversible upon subsequent cycles of UV and visible light irradiations. In the absence of visible light,

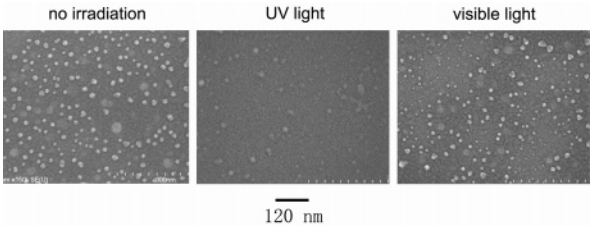

Figure 8. SEM images of core−shell micelles of PAzoMA-*b*-PAA (6) formed by adding water in dioxane solution: before irradiation and after UV and visible light irradiation. The initial polymer concentration was 1.0 mg/mL.

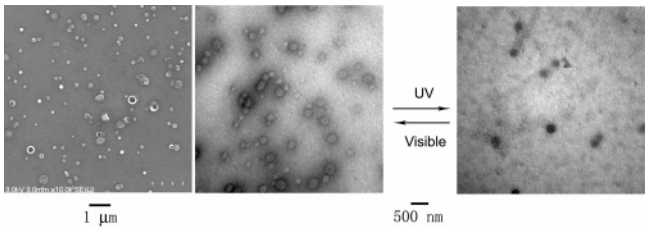

Figure 9. SEM (left) and TEM (right) images showing vesicles of PAzoMA-*b*-PAA (6) formed by adding water in dioxane solution, and the light-induced reversible change in the aggregate morphology. The initial polymer concentration was 1.0 mg/mL.

thermal relaxation of the cis isomer of this azobenzene mesogen is slow, needing hours to complete. Note also that the photoisomerization of azobenzene under UV and visible light resulted in no change in the optical density at 700 nm used for the turbidity measurement, which further ensures that the turbidity change in Figure 6 is due to changes in light scattering determined by the aggregates.

We also used PAzoMA-*b*-PAA (6) to investigate the formation of micellar aggregates and their response to alternating UV and visible light illumination. As compared to PAzoMA-*b*-PAA (3), this diblock copolymer has not only a much longer hydrophobic block with about 74 units of AzoMA, but also a hydrophilic block composed of about 22 units of AA and 46 units of *t*BA due to the lower hydrolysis degree (Table 1), which further shifts the hydrophobic-to-hydrophilic balance by reducing the hydrophilicity of the hydrophilic block. Using the initial polymer concentration of 1.0 mg/mL in dioxane, the addition of 9% of water resulted in the formation of polymeric core−shell micelles (average diameter around 15 nm), as can be seen from the SEM image in Figure 8. After 10 min UV light illumination of the solution, the number of micelles diminished drastically (most parts of the cast samples actually showed the absence of micelles). However, following the subsequent 3 min visible light illumination of the solution, core−shell micelles reappeared in the cast samples. Moreover, when 15% of water was added in the dioxane solution, PAzoMA-*b*-PAA (6) formed vesicles that also displayed reversible changes on alternating UV and visible light illumination. Figure 9 shows the SEM and TEM images of samples cast from the same micellar solution. Micellar aggregates in the form of vesicles are visible on both microscopes. The various sizes for the vesicles (mostly in the range of 100−300 nm) are likely caused by the relatively large polydispersity of PAzoMA-*b*-PAA (6). Likewise, after UV light irradiation of the solution, vesicles essentially disappeared; only some micelle-like large aggregates (∼200 nm) could be observed. On subsequent visible light irradiation, vesicles were reformed in the solution. The results obtained using PAzoMA-*b*-PAA (6) show unambiguously the severe disruption of both polymeric core−shell micelles and vesicles in the solution under UV light illumination and the recovery of those micellar aggregates after the visible light illumination of the solution. Again, the reversible change by switching the wavelength of light in the UV and visible region indicates that the photoisomerization of azobenzene mesogens of the PAzoMA block is at the origin of the response of the micellar aggregates to the optical stimulus.

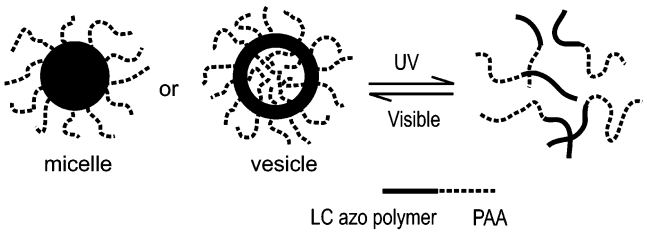

Figure 10. Schematic illustration of the disruption and reformation of polymeric core−shell micelles and vesicles of PAzoMA-*b*-PAA on alternating UV and visible light illumination.

On the basis of the above observations, the behavior of light-responsive micellar aggregates formed by amphiphilic diblocks containing an LC azobenzene polymer is schematically recapitulated in Figure 10. Basically, it appears that both polymeric core−shell micelles and vesicles could be disrupted and reformed in solution upon alternating UV and visible light irradiation as a result of the reversible trans−cis photoisomerization of azobenzene mesogens on the hydrophobic block that aggregates into the compact core or membrane regions. The results support the anticipated optical plasticization effect on the aggregated PAzoMA block. Under UV light, the trans−cis isomerization induces the LC-to-isotropic phase transition, which makes the aggregates mechanically weaker, more easily deformable, and disintegrable. Stirring the solution may play a role in the process because it may provide a shear force that helps break the micellar aggregates with azobenzene mesogens in the cis form. Under visible light, since azobenzene mesogens regain the elongated trans conformation, the thermodynamically stable micellar aggregation state before UV irradiation is recovered. Although the used azobenzene mesogen has near 100% trans−cis isomerization on UV light irradiation (Figure 7), a very high efficiency for photoisomerization may not be necessary if the LC-to-isotropic phase transition is indeed responsible for the strong disruption effect on micellar aggregates, because for LC phases formed by azobenzene mesogens, a partial photoisomerization may be enough to destabilize the LC phases. Detailed investigations on the mechanisms of optical control of polymeric micellar aggregates are underway, and the results will be reported in due course.

Conclusions

We report a synthetic method for the preparation of light-responsive amphiphilic diblock copolymers composed of a hydrophilic block of PAA and a hydrophobic block of PAzoMA. It consists of preparing a diblock copolymer of PAzoMA-*b*-P*t*BA through ATRP and then selectively hydrolyzing the P*t*BA block to yield PAzoMA-

b-PAA. As a result of the reversible trans−cis photoisomerization of azobenzene mesogens in the PAzoMA block, reversible changes in morphology of the micellar aggregates formed by adding water in dioxane solution of PAzoMA-*b*-PAA were observed under alternating UV and visible light irradiation. The study suggests that the use of a side-chain liquid crystalline polymer containing an azobenzene mesogenic unit may be a way to design amphiphilic diblock copolymers whose micellar aggregates can be strongly disrupted by light due to the optical plasticization effect related to the photochemical phase transition of azobenzene mesogens in the compact region of aggregates.

Acknowledgment. Financial support from the Natural Sciences and Engineering Research Council of Canada and le Fonds québécois de la recherche sur la nature et les technologies of Québec is acknowledged.

References and Notes

(1) See, for example: (a) Zhang, L.; Eisenberg, A. *Science* **1995**, *268*, 1728. (b) Honda, C.; Sakaki, K.; Nose, T. *Polymer* **1994**, *35*, 5309. (c) Liu, G.; Qiao, L.; Guo, A. *Macromolecules* **1996**, *29*, 5508. (d) Jenekhe, S. A.; Chen, X. L. *Science* **1998**, *279*, 1903. (e) Massey, J.; Power, K. N.; Manners, I.; Winnik, M. A. *J. Am. Chem. Soc.* **1998**, *120*, 9533. (f) Won, Y.-Y.; Davis, H. T.; Bates, F. S. *Science* **1999**, *283*, 960. (g) Discher, B. M.; Hammer, D. A.; Bates, F. S.; Discher, D. E. *Curr. Opin. Colloid Interface Sci*. **2000**, *5*, 125. (h) Sommerdijk, N. A. J. M.; Holder, S. J.; Hiorns, R. C.; Jones, R. G.; Nolte, R. J. M. *Macromolecules* **2000**, *33*, 8289. (i) Du, J.; Chen, Y. *Macromolecules* **2004**, *37*, 5710.

(2) See, for example: (a) Groenewegen, W.; Egelhaaf, S. U.; Lapp, A.; van der Maarel, J. R. C. *Macromolecules* **2000**, *33*, 3283. (b) Ravi, P.; Wang, C.; Tam, K. C.; Gan, L. H. *Macromolecules* **2003**, *36*, 173.

(3) See, for example: (a) Zhang, L.; Eisenberg, A. *Macromolecules* **1996**, *29*, 8805. (b) Lee, A. S.; Buetuen, V.; Vamvakaki, M.; Armes, S. P.; Pople, J. A.; Gast, A. P. *Macromolecules* **2002**, *35*, 8540.

(4) Napoli, A.; Valentini, M.; Tirelli, N.; Muller, M.; Hubbell, J. A. *Nat. Mater.* **2004**, *3*, 183.

(5) See, for example: (a) Discher, D. E.; Eisenberg, A. *Science* **2002**, *297*, 967. (b) Haag, R. *Angew. Chem., Int. Ed*. **2004**, *43*, 278.

(6) Orihara, Y.; Matsumura, A.; Saito, Y.; Ogawa, N.; Saji, T.; Yamaguchi, A.; Sakai, H.; Abe, M. *Langmuir* **2001**, *17*, 6072.

(7) Einaga, Y.; Sato, O.; Iyoda, T.; Fujishima, A.; Hashimoto, K. *J. Am. Chem. Soc.* **1999**, *121*, 3745.

(8) Bai, S.; Zhao, Y. *Macromolecule*s **2001**, *34*, 9032.

(9) Leclair, S.; Mathew, L.; Giguere, M.; Motallebi, S.; Zhao, Y. *Macromolecules* **2003**, *36*, 9024.

(10) Zhao, Y.; Tong, X. *Adv. Mater.* **2003**, *15*, 1431.

(11) Cui, L.; Zhao, Y. *Chem. Mater.* **2004**, *16*, 2076.

(12) Choucair, A.; Eisenberg, A. *Eur. Phys. J.* **2003**, *E 10*, 37.

(13) Ikeda, T.; Tsutsumi, O. *Science* **1995**, *268*, 1873.

(14) Blanche, P.-A.; Lemaire, P. C.; Dumont, M.; Fischer, M. *Opt. Lett.* **1999**, *24*, 1349.

(15) Davis, K. A.; Matyjaszewski, K. *Macromolecules* **2000**, *33*, 4039.

(16) Ringsdorf, H.; Schmidt, H. W. *Makromol. Chem.* **1984**, *185*, 1327.

(17) (a) George, A. O.; Gao, L.; Paul, V. *J. Am. Chem. Soc.* **1977**, *99*, 968. (b) Henselwood, F.; Liu, G. *Macromolecules* **1997**, *30*, 488. (c) Qi, Z.; Edward, E. R.; Karen, L. W. *J. Am. Chem. Soc.* **2000**, *122*, 3642.

(18) Zhang, L.; Eisenberg, A. *Macromolecules* **2000**, *33*, 2561.

(19) Paul, J. Y. L.; Painter, C.; Coleman, M. M. *Macromolecules* **1988**, *21*, 954.

(20) Walther, M.; Faulhammer, H.; Finkelmann, H. *Macromol. Chem. Phys.* **1998**, *199*, 223.

(21) Cui, L.; Zhao, Y.; Yavrian, A.; Galstian, T. *Macromolecules* **2003**, *36*, 8246.

MA048416A